Friction **12**(6): 1272–1282 (2024)
https://doi.org/10.1007/s40544-023-0814-y
ISSN 2223-7690
CN 10-1237/TH

RESEARCH ARTICLE

Bayesian inference-based wear prediction method for plain bearings under stationary mixed-friction conditions

Florian KÖNIG[1,*], Florian WIRSING[1], Georg JACOBS[1], Rui HE[2], Zhigang TIAN[2], Ming J. ZUO[2,3]

[1] *Institute for Machine Elements and Systems Engineering, RWTH Aachen University, Aachen 52062, Germany*

[2] *Department of Mechanical Engineering, University of Alberta, Edmonton T6G1H9, Canada*

[3] *Qingdao International Academician Park Research Institute, Qingdao 266000, China*

Received: 17 April 2023 / Revised: 16 June 2023 / Accepted: 07 August 2023

Abstract: This study introduces a method to predict the remaining useful life (RUL) of plain bearings operating under stationary, wear-critical conditions. In this method, the transient wear data of a coupled elastohydrodynamic lubrication (mixed-EHL) and wear simulation approach is used to parametrize a statistical, linear degradation model. The method incorporates Bayesian inference to update the linear degradation model throughout the runtime and thereby consider the transient, system-dependent wear progression within the RUL prediction. A case study is used to show the suitability of the proposed method. The results show that the method can be applied to three distinct types of post-wearing-in behavior: wearing-in with subsequent hydrodynamic, stationary wear, and progressive wear operation. While hydrodynamic operation leads to an infinite lifetime, the method is successfully applied to predict RUL in cases with stationary and progressive wear.

Keywords: plain bearings; wear modeling; remaining useful life prediction; Bayesian inference

1 Introduction

Plain bearings are widely used in drivetrains because of their high load-carrying capacity, low space requirements, and good damping properties. New fields of application such as in wind turbines [1] and changed operating strategies such as automatic start-stop [2] as well as pulse-and-glide strategies [3] cause an increased proportion of low sliding speeds, which may prevent a sufficient hydrodynamic film formation in the bearings, leading to boundary or mixed-friction conditions. Furthermore, the use of low-viscosity oils and water for an efficient and environmentally acceptable lubrication (EAL) becomes more prominent, e.g. for marine propulsion systems [4–7], which results in a decrease of load-carrying capacity and thereby also in an increased risk of mixed-friction conditions. At such operation conditions, a plain bearing may be subject to high friction and wear, which affects the bearing behavior [7–13] and limits the service life [14]. Consequently, the reliability of a plain bearing due to mixed-friction conditions is a potential limiting factor in a drivetrain [15, 16]. Previous studies on failure modes of internal combustion engines show that an engine failure due to abrasive wear in plain bearings is a dominant cause of failure [14]. From a tribological point of view, mild abrasive wear typically leads to continuous degradation of the bearing shell, resulting in a continuous decrease of its remaining useful lifetime (RUL). In contrast, abnormal operational conditions, e.g. due to starved lubrication, may lead to an abrupt failure due to severe abrasive or adhesive wear [12, 17], which are not part of the regular continuous degradation during a bearing lifetime.

For the specific purpose of RUL prediction of plain bearings subjected to mild abrasive wear, previous works concluded that the wear limit of a plain bearing

* Corresponding author: Florian KÖNIG, E-mail: florian.koenig@imse.rwth-aachen.de

can be defined by the permissible wear depth h_{limit}, permissible contact angle α_{limit} as well as permissible wear volume W_{limit}, see Fig. 1.

These are chosen as criteria at which the properties of the sliding layer can still be considered unchanged. The increase of the diametrical clearance *C*, characterized by the difference between the bearing diameter and the shaft diameter, can be used as a criterion. From this criterion, a maximum for the permissible wear depth h_{limit} can be derived. For dynamically loaded bearings, the permissible wear depth h_{limit} should not exceed 25% [18] to 50 % [11] of the initial bearing clearance ($h_{\text{limit}} = 0.5C$). For stationary loaded bearings, 40% are acceptable without a major change of operational behavior [19]. The permissible contact angle α_{limit} should not exceed values of 100 to 110 [20]. In contrast, no design guidelines are available for the permissible wear volume W_{limit}, which somewhat considers the bearing dimensions, wear angle, and wear depth. Therefore, a system-dependent W_{limit} should be considered as a suitable alternative. The prognosis of bearing wear is commonly conducted with coupled mixed-elastohydrodynamic (mixed-EHL) and wear simulations [21, 22]. However, for the forecasting of bearing wear during operation, less computationally expensive surrogate or meta models have been developed. For this purpose, recurrent neural networks [23–25], which are generally employed for time-series forecasting, or time-delay neural networks [26] are potential solutions. In previous works, we employed long-short-term-memory (LSTM) neural networks. For the training of the LSTM, a mixed-EHL and wear simulations were employed to learn the correlation between radial load, temperature, speed, friction coefficient as input and wear volume as output. The approach was successfully applied on a plain bearing test rig [24].

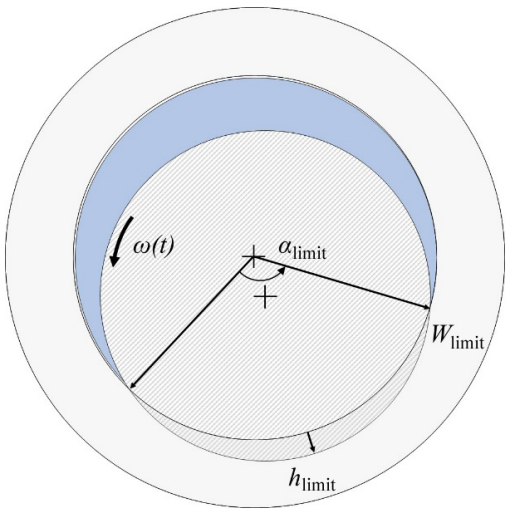

Fig. 1 Sketch of the criteria for a plain bearing's wear lifetime.

Bote-Garcia et al. [27] developed a wear prediction method for plain bearings that uses acoustic emission data and machine learning methods; namely, linear regression, random forest regressor, multilayer perceptron, and recurrent neural networks were applied. The wear volume has been estimated with a root mean square error of 0.32 mm^3 and a coefficient of determination of 93%. Shutin et al. [28] used a combination of physics-based simulations and neural networks for bearing RUL and wear prediction in locomotive traction motor axle bearings.

However, as of today, the prediction of the wear-induced RUL of a plain bearing is a major challenge. The reasons for this are twofold. On the one hand, selecting suitable degradation indicators is not straightforward because the failure thresholds for common measured variables, e.g. temperature or vibration, are often unknown. Particularly, this is the case when historical data of comparable systems is limited. On the other hand, the direct use of physically meaningful degradation indices, such as wear volume or depth as indices, is difficult, since these physical indices often cannot be measured directly.

The core idea to overcome these limitations is to extend an existing physics-based wear simulation of a plain bearing towards the analysis of the RUL using a statistical degradation model based on Bayesian inference [29]. Bayesian-inference models allow the model parameters to be updated based on actual measurements and therefore always track wear behavior without model pre-training, even if it deviates from expectations. This is of particular interest since the wear behavior in a complex mechanical system may change over time due to varying conditions. As a first step, the purpose of this study is to show the suitability of this approach for plain bearing wear prediction. Therefore, simulations of different stationary, mixed-friction operating conditions were conducted and compared to the experimental test rig results obtained under similar operating conditions. Subsequently, the RUL was calculated for different

stationary, mixed-friction operating conditions using the statistical reliability model.

2 Materials and methods

To follow this idea, plain bearing experimental and physics-based simulation results of previous works [22, 30], which are briefly summarized in Section 2.1, were further analyzed and evaluated. Subsequently, the wear simulation results were used to parametrize the statistical degradation model introduced in Section 2.2.

2.1 Bearing wear experiments and physics-based simulations

The onset of this study are bearing wear experiments on a model test rig with bronze plain bearings made of CuSn12NiC-GCB. Three sets of experiments were conducted with different stationary operational conditions in terms of load and temperature as well as a varying number of shaft revolutions. Each experiment was conducted in duplicate. In each set, the number of shaft revolutions was varied between 30,000, 360,000, and 720,000, while the rotational speed was set to 250 min^{-1}. Consequently, the duration of the short experiments in each set was 2 hours, whereas the bearing was operated for 48 hours in the longest experiments. The operating conditions, which have been chosen based on the experience of previous experiments with similar specimens [22], are summarized in Table 1.

After each experiment, the wear pattern, viz. the location and severity of wear, in a plain bearing was analyzed using a form tester MarForm MMQ 100 with probe T2W (Mahr, Göttingen, Germany). Similar to our previous works, the contour of a new and worn plain bearing was measured in multiple equally distributed positions across the bearing width, which is exemplarily shown in Fig. 2. In this study, a total number of 10 positions was measured prior and post testing. Subsequently, the wear volume was calculated via numerical integration [22].

To obtain transient wear data, a mixed-EHL simulation model of the plain bearing was built up in AVL Excite Power Unit. For the reader's convenience, this is shortly summarized. The model consists of a rotating steel shaft and a flexible bronze bearing, whose dimensions and material properties are identical to the experimental setup. Furthermore, the local mixed friction intensity is considered with a generic friction

Table 1 Properties of the used lubricant and summarized testing parameters.

	Running-in test series A	Running-in test series B	Running-in test series C
Lubricant		FVA 2	
Kinematic viscosity (40 °C) ($mm^2 \cdot s^{-1}$)		32	
Kinematic viscosity (100 °C) ($mm^2 \cdot s^{-1}$)		5.35	
Testing parameters			
Shaft roughness Ra (μm)	0.25	0.25	0.25
Bearing temperature (°C)	40	80	64
Oil inlet temperature (°C)	30	70	54
Operational viscosity (mPa·s)	27	7.2	11.5
Oil inlet pressure (bar)	3	3	3
Radial load (N)	2,250	2,250	3,600
Specific pressure ($N \cdot mm^{-2}$)	5	5	8
Rotational speed (min^{-1})	250	250	250
Sliding velocity ($m \cdot s^{-1}$)	0.392	0.392	0.392
Sommerfeld number (–)	19.6	75	75
Test time (h)	2; 24; 48	2; 24; 48	2; 24; 48
Runtime / shaft revolutions	30,000; 360,000; 720,000	30,000; 360,000; 720,000	30,000; 360,000; 720,000

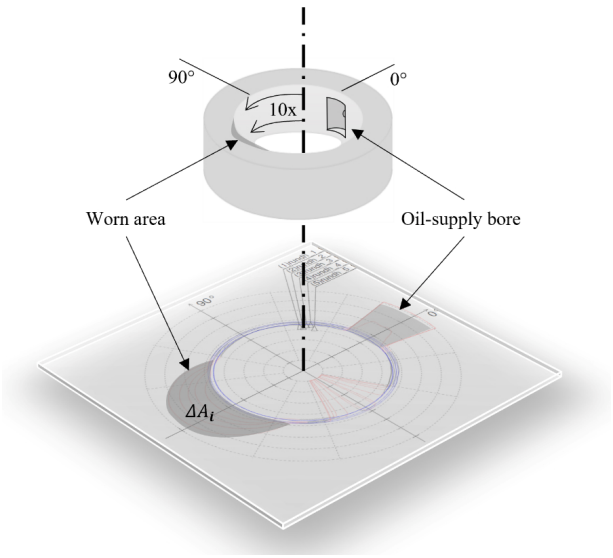

Fig. 2 Bearing contour analysis: The worn area is located at the bottom-left side whereas the oil-supply bore is located at the right side.

model [31]. The bearing loads are accumulated into a severity factor. Subsequently, the energetic wear law according to Fleischer is used to calculate the macroscopic wear. In each simulation step, a maximum permissible wear depth of 0.125 μm is set, thereby setting the runtime between two simulations. Furthermore, the wear-induced changes of the surface topography are considered by adapting the input surfaces for the asperity contact model in the mixed-EHL simulation. Consequently, the effect of a transient change of mixed-friction intensity throughout the bearing lifetime can be considered [22].

2.2 Model-based RUL prediction

As motivated in Ref. [32], where the contact pressure and Archard's wear law are used within a data-driven degradation model, the target is to predict the RUL of plain bearings subjected to the abrasive wear failure. The proposed degradation model is based on a linear degradation model, see Eq. (1). It should be noted that such a model can be used since the condition monitoring data, i.e., experimental or simulation data, is available and the system-specific damage criterion is known. The choice of a permissible wear volume as a damage criterion is typical from a reliability engineering point of view, however, in engineering practice, the definition of a permissible wear depth or angle can be more appropriate as stated in the introduction. Nevertheless, the permissible wear volume W_{limit} has been chosen as a damage criterion on the basis of empirical knowledge of the given bearing system. Consequently, the simulated wear volume, which is determined in the coupled mixed-EHL and wear simulations, forms the condition indicator of the degradation model. The degradation model is used to predict future degradation development. Specifically, the future wear volume V_{t+t_k} in Eq. (1) is predicted based on past information about the simulated wear volume V_t. This makes it possible to predict when the condition indicator will reach the specified threshold, allowing the system's RUL to be estimated. Also, the use of a linear degradation model implies that the continuous rubbing causes solely abrasive wear.

$$V_{t+t_k} = V_t + \beta_t t_k + \varepsilon \tag{1}$$

where V_{t+t_k} is the predicted wear volume at runtime $t+t_k$. The model parameter β_t at runtime t follows the normal distribution $N(m_t, \sigma_t)$ and for runtime $t = t_0$ the model parameter β_0 follows the normal distribution $N(m_0, \sigma_0)$. The error term ε also follows a normal distribution $N(0, \tau)$. A threshold for the degradation parameter must be defined according to the permissible wear values described in Section 1. In this study, the limit for the permissible wear volume W_{limit} was chosen and set to $D = 1.416$ mm^3, which marks the maximum value of the physical simulation of test series B. It should be noted that this value is thereby chosen on the basis of empirical knowledge for the given bearing system.

The prediction of the RUL can be continuously updated at each step using Bayesian inference until the calculated wear volume threshold is reached. According to Eq. (2), the increment in wear volume between two consecutive steps is defined as L_{t+t_k}.

$$L_{t+t_k} = V_{t+t_k} - V_t \tag{2}$$

At runtime $t+t_k$, given the observed wear volume V_{t+t_k}, the posterior distribution of β_{t+t_k} can be evaluated by Eq. (3), using Bayesian inference [33]. The method is briefly explained in Eq. (3).

$$f_{\text{post}}\left(\beta_{t+t_k} \mid V_{t+t_k}\right) \propto l\left(V_{t+t_k} \mid \beta_t\right) f_{\text{pri}}\left(\beta_t\right)$$

$$\propto \exp\left[-\frac{1}{2\tau^2}\left(L_{t+t_k}-\beta_t t_k\right)^2\right]\times\exp\left[-\frac{1}{2\sigma_t^2}\left(m-m_t\right)^2\right]$$
$$=\exp\left[-\frac{1}{2\tau^2}\left(L_{t+t_k}^2+\beta_t^2 t_k^2-2L_{t+t_k}\beta_t t_k\right)\right]$$
$$\times\exp\left[-\frac{1}{2\sigma_t^2}\left(m^2+m_t^2-2mm_t\right)\right] \tag{3}$$

where $f(\beta_t)$ is the prior distribution of β_t, i.e., $N(m_t,\sigma_t)$, and $l(V_{t+t_k}|\beta_t)$ is the likelihood function at runtime $t+t_k$. Since the posterior distribution $f_{\text{post}}(\beta_{t+t_k}|V_{t+t_k})$ also follows a normal distribution $N(m_{t+t_k},\sigma_{t+t_k})$, Eq. (4) can be derived.

$$f_{\text{post}}(\beta_{t+t_k}|V_{t+t_k})$$
$$\propto \exp\left[m^2\left(-\frac{1}{2\tau^2}t_k^2-\frac{1}{2\sigma_t^2}\right)+m\left(\frac{m_t}{\sigma_t^2}+\frac{L_{t+t_k}t_k}{\tau^2}\right)-\left(\frac{L_{t+t_k}^2}{2\tau^2}+\frac{m_t^2}{2\sigma_t^2}\right)\right]$$
$$=\exp-\frac{1}{2\sigma_{t+t_k}^2}\left(m^2-2mm_{t+t_k}+m_{t+t_k}^2\right)$$
$$=\exp\left[-\frac{1}{2\sigma_{t+t_k}^2}\left(m-m_{t+t_k}\right)^2\right] \tag{4}$$

Based on Eqs. (3) and (4), the parameters of the posterior distribution of β_{t+t_k} can be evaluated using Eqs. (5) and (6). Hence, these values are updated for each subsequent step on the basis of the current step.

$$\sigma_{t+t_k}^2=\frac{\tau^2\sigma_t^2}{\sigma_t^2 t_k^2+\tau^2} \tag{5}$$

$$m_{t+t_k}=\sigma_{t+t_k}^2\left(\frac{m_t}{\sigma_t^2}+\frac{L_{t+t_k}t_k}{\tau^2}\right) \tag{6}$$

For a heuristically chosen, initial $m_0=10^{-8}$ and $\sigma_0=10^{-4}$, it is possible to observe V_{t+t_k} at runtime $t+t_k$. Then, L_{t+t_k} can be calculated to update $\sigma_{t+t_k}^2$ and m_{t+t_k}, respectively, based on σ_t^2 and m_t obtained at runtime t with Eqs. (5) and (6). It should be noted that L_{t+t_k} is positive at all times. However, σ_t^2 can be subjected to change, therefore a posterior mean of the model parameter β, i.e., m_{t+t_k} can decrease or increase compared to m_t according to the change of the wear volume. At runtime t, the wear volume at a specific point of runtime t_k in the future can be predicted based on β_t by Eq. (7).

$$\hat{V}_{t+t_k}=V_t+\beta_t t_k+\varepsilon \tag{7}$$

where V_t is the observed volume at runtime t, and $\hat{V}_{t+t_k}$ is the predicted wear volume at runtime $t+t_k$. In contrast to V_{t+t_k} in Eq. (1), $\hat{V}_{t+t_k}$ in Eq. (7) indicates that the wear volume is unknown and thereby estimated during the Bayesian updating process. The mean $\mu_{v,t+t_k}$ and variance $\sigma_{v,t+t_k}$ of the predictive distribution of $\hat{V}_{t+t_k}$ are given by Eqs. (8) and (9).

$$\mu_{v,t+t_k}=V_t+m_t t_k \tag{8}$$

$$\sigma_{v,t+t_k}^2=\tau^2+\sigma_t^2 t_k^2 \tag{9}$$

The predictive distribution of $\hat{V}_{t+t_k}$ is used to compute the distribution of the remaining useful life T_r. For this purpose, the predetermined failure threshold D, which is associated with the wear volume, is obtained using Eq. (10). At runtime $t=T_r$, $\hat{V}_{t+T_r}=D$. Thus, the probability density function (PDF) for the RUL can be calculated by determining the probability that the wear volume at runtime $t+t_k$ is higher than D.

$$P\left(T_r\leqslant t_k\,|\,V_t\right)=P\left(V_{t+t_k}\geqslant D\,|\,V_t\right)$$
$$=1-P\left(V_{t+t_k}\leqslant D\,|\,V_t\right)$$
$$=1-P\left(Z\leqslant\frac{D-\mu_{v,t+t_k}}{\sigma_{v,t+t_k}}\right)$$
$$=\Phi\left(\frac{\mu_{v,t+t_k}-D}{\sigma_{v,t+t_k}}\right) \tag{10}$$

where $\Phi(\cdot)$ is the cumulative density function of a standardized normal random variable Z. Hence, the cumulative density function $\Phi(\cdot)$ is calculated using the statistical parameters $\mu=0$ and $\sigma=1$. With this method, it is possible to calculate the PDF throughout the lifetime of a technical system. Further information on this process can be found in Ref. [34].

3 Results and discussion

Plain bearing experiments and coupled mixed-EHL and wear simulations were conducted to study the wear behavior under three mixed-friction conditions

listed in Table 1. The results of the wear simulation and the measured wear volumes are compared in Fig. 3. For test series A, the wear volume increases significantly within the first 30,000 shaft revolutions. After this initial run-in wear, experiments show no further increase in wear volume. After approx. 120,000 shaft revolutions, the simulation model predicts an infinite lifetime. The different step sizes between two simulation steps are related to the fixed maximum wear depth per coupled mixed-EHL and wear simulation as introduced in Ref. [22]. The reason for this is the additional load-carrying capacity of the plain bearing as a result of the running-in process. As can be seen in Fig. 3(b), the number of simulation steps is high during the running-in phase, which is necessary to accurately capture the wearing-in of the surface topography. In test series B, the wear volume increases within the first 30,000 shaft revolutions with a higher wear rate than in test series A. Subsequently, experiments and simulations show a significantly decaying wear rate between 30,000 and 360,000 shaft revolutions. Between 360,000 and 720,000 shaft revolutions, a progressive development of the wear volume can be observed. This can be explained by the increasing conformity between the shaft and plain bearing, which leads to a decrease in load-carrying capacity and results in a higher mixed friction intensity. Also, the number of simulation steps increases due to a low number of shaft revolutions to reach a fixed maximum wear depth of 0.125 μm per step. In test series C, the wear volume grows within the first 30,000 shaft revolutions at a higher wear rate than in test series A and B. Subsequently, experiments and simulations show a clearly decaying wear rate between 30,000 and 720,000 shaft revolutions with an approximately linear development of the wear volume [30], which is also in agreement with other works [13, 35]. In all experiments and simulations, derivations at 30,000 shaft revolutions can be observed. The reason for this is twofold. Firstly, tolerances in surface roughness, cylindricity can lead to deviations between the physics-based model and the distribution of experimental results. Secondly, the radial load is applied and increased within the first minute after the initial start of the rotation. This kind of dynamic effect could potentially affect the wear pattern as well as the temperature distribution in the bearing, especially in cases with high temperatures and loads.

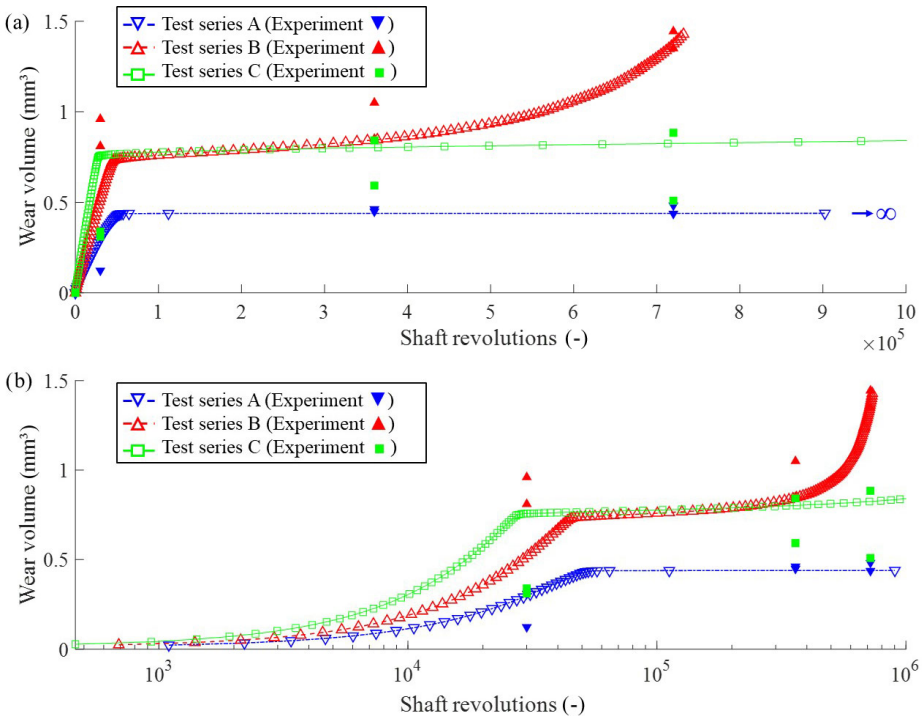

Fig. 3 Wear volume evolution: Wear volume evolution of running-in test series A to C. The markers indicate the number of simulation steps in the physics-based simulation model: (a) linear scaled runtime, (b) log-scaled runtime. Reproduced with permission from Ref. [30], © Verlag Mainz, 2020.

In the following section, Bayesian inference-based RUL prognostics are conducted. To predict the RUL, the previous physics-based wear simulations were fitted into the linear degradation model according to Eq. (1). The simulated wear volume V_t is the input variable for the linear degradation model. The remaining model parameters according to Eq. (1) are continuously updated by the statistical approach using Bayesian inference to predict the future wear volume V_{t+t_k}. Hence, the physics-based wear simulation results are translated into a statistical, mathematical problem. The wear simulation result of test series B is compared to the predicted wear volume in Fig. 4. The prediction generally agrees very well with the simulation results. A deviation between the simulation result and prognosis can be observed in the transition from running-in wear to operational wear. This deviation is due to the chosen approach and the high gradient change, which cannot be accurately captured in the statistical model. This can be explained by the updated mean and variance in each step. As introduced in Section 2.2, these values are calculated from the data of the previous step (Eqs. (5) and (6)).

The PDF for the failure runtime of the plain bearing, is shown in Fig. 5, where a dashed line indicates the corresponding number of shaft revolutions, at which the physics-based wear simulation crosses the predefined threshold value of suitable wear volume. The area between the abscissa and the curve corresponds to the probability. Figure 5(a) shows an overview and maps both the running-in and the subsequent wear. Figure 5(b) corresponds to a detailed view of Fig. 5(a), where only the running-in wear is shown. Due to the rather constant wear rate, i.e., close-to-linear wear progress over multiple simulation steps, as shown in Fig. 3(a), the failure runtime for the simulation steps 10–40 converges to a rather distinct lifetime prediction, which can be recognized by the high peak value of the PDF and the low variance. However, as observed in the results of the physics-based simulations (Fig. 3), this marks the transition from running-in to steady-state wear. Hence, at step 50, which is also included in Fig. 5(b), the predicted failure runtime and fuzziness increases significantly. However, as shown in Fig. 5(c), the predicted failure runtime at step 90 onwards decreases again due to the transition from stationary to progressive wear. Eventually, the lifetime converges to a fixed value, see Fig. 5(c). With decreasing difference between the condition indicator and the damage criterion, a smaller span and larger PDF can be observed, which leads to a more accurate RUL prognosis.

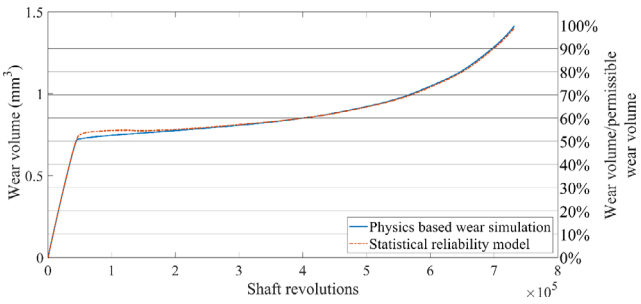

Fig. 4 Comparison of the predicted wear volume to the simulation data of test series B.

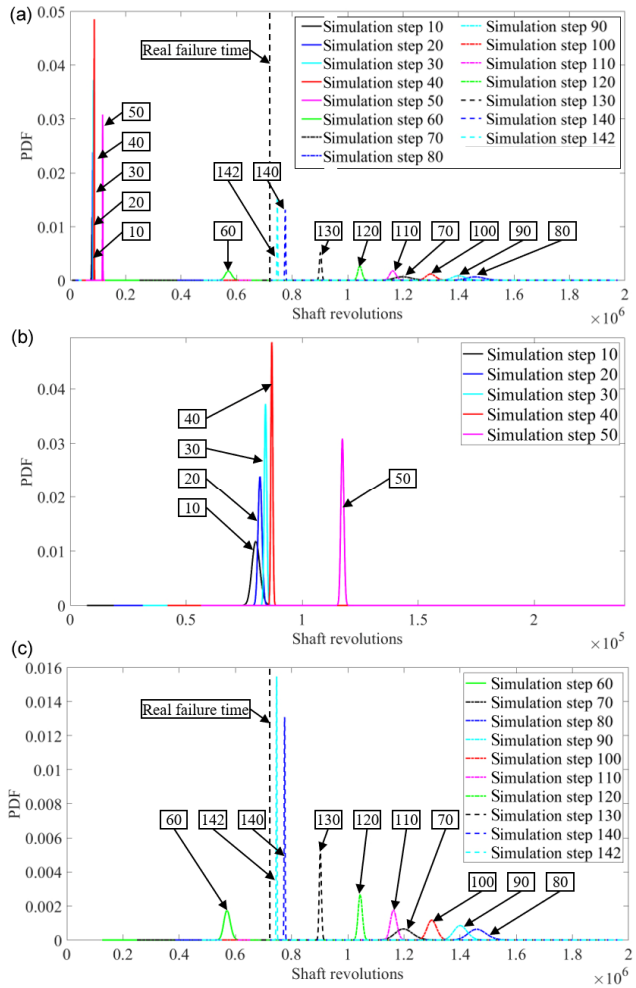

Fig. 5 PDF of the predicted bearing lifetime of test series B. (a) Full wear lifetime evolution, (b) running-in period, and (c) stationary and progressive wear period.

For the conditions of test series C, a good agreement between physics-based simulation and the statistical reliability model can be achieved. As can be seen in Fig. 6 at approximately 50,000 shaft revolutions, there is an overshoot in the signal at the transition from running-in wear to operational wear. Similar to test series B, this can be explained by the stepwise update of the statistical model, which cannot follow the strong change in the gradient of the numerical model.

The PDF for test series C is shown in Fig. 7, where the same classification as for test series B is used. Figure 7(a) shows the lifetime prognosis for both wear cases, whereas Fig. 7(b) shows the life for running-in wear and Fig. 7(c) shows the life for subsequent stationary wear. Similar to the running-in in test series B, the RUL firstly converges towards a fixed value, as shown in Fig. 7(b). Subsequently, the RUL increases again due to the decreasing wear rate after wearing-in as shown in Fig. 7(c). The predicted failure runtime at step 75 is approximately 8.3×10^6 shaft revolutions or 23.1 days.

As can be seen in Fig. 7, test series C does not represent the entire wear lifetime of the plain bearing. Similar to test series B, approximately 50% of the permissible wear occurred during the running-in, which is occurring within the first 40 simulation steps. During the subsequent stationary wear regime, the ratio between wear volume and threshold reaches 58% at simulation step 75. Furthermore, it can be seen that the statistical approach leads to comparable results with the physics-based wear simulation. Hence, the application of a statistical reliability model with the assumption of linear degradation is valid for the particular use case of steady-state operated plain bearings. In the future, the idea is to replace the physics-based simulations with other condition indicators that can be used for condition monitoring of bearing systems. During running-in and progressive wear, cumulative damage has a significant effect on the degradation rate. Cumulative damage may accelerate or decelerate the variation frequency of the degradation process. Since false predictions during the running-in period can only be ignored by the knowledge of the system, future research should also consider the potential use of exponential degradation models, which can better characterize situations where the degradation rate changes sensitively. This is not limited to running-in but can also include dynamic load or speed cycles.

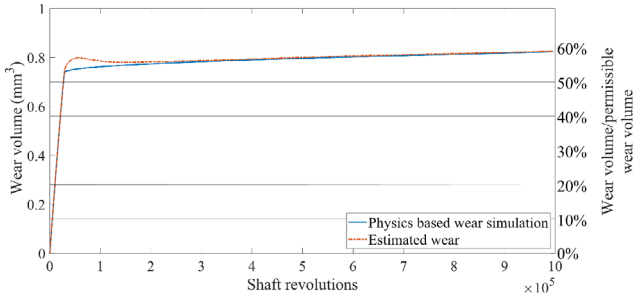

Fig. 6 Comparison of the predicted wear volume to the simulation data of test series C.

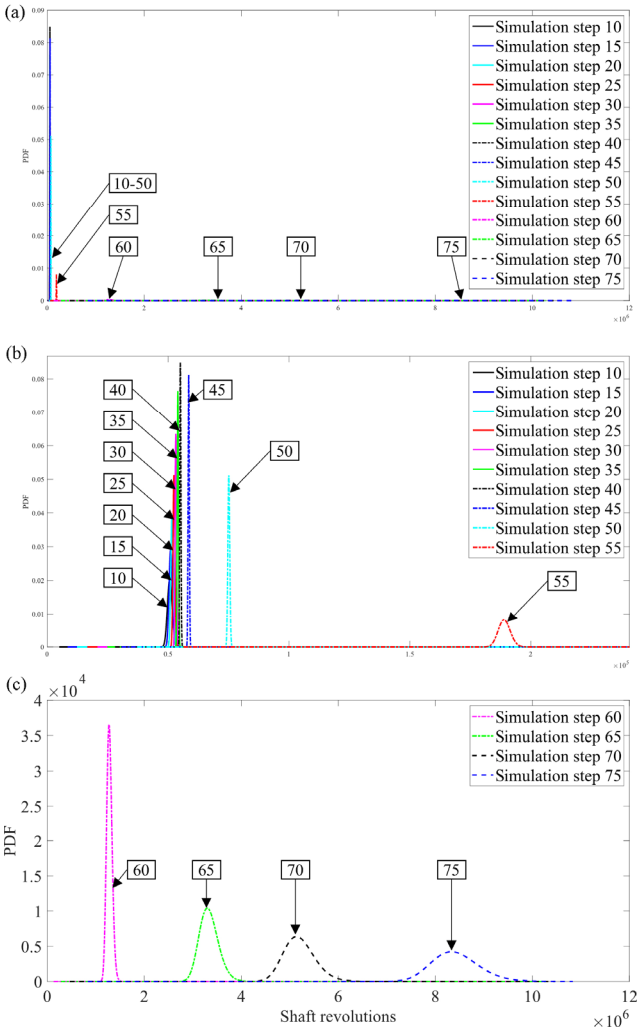

Fig. 7 PDF of the predicted bearing lifetime of test series C. (a) Full wear lifetime evolution, (b) running-in period, and (c) stationary wear period

4 Conclusions

The aim of this study was to predict the remaining useful life (RUL) of plain bearings operating under different stationary, mixed-friction conditions. Due to the non-stationary wear behavior of plain bearing, a numerical simulation approach based on coupled mixed-elastohydrodynamic (mixed-EHL) and wear simulations was linked to a degradation model based on Bayesian inference.

For validation of the proposed method, multiple plain bearing experiments under mixed-friction conditions were conducted. On the basis of the results obtained, the following conclusions can be drawn:

1) Depending on the operational conditions, plain bearing may show an initial operation in mixed friction. After wearing-in, the bearing may operate in a wear-free hydrodynamic regime or within a mixed-friction regime with either stationary or progressive wear. A linear degradation model can be used to model these transitions with reasonable accuracy.

2) With the statistical reliability model based on Bayesian inference, it is possible to estimate the RUL throughout the non-stationary wear progression of a plain bearing system. Changes in the wear rate throughout the bearing lifetime can be considered due to the continuous updating of the RUL.

Future works will focus on elucidating the benefits of the proposed method compared to previously reported methods. Also, the combination with condition monitoring systems and machine learning methods is possible and thereby replaces the time-consuming mixed-EHL and wear simulations for real-time wear prognosis.

Acknowledgements

This work was funded by the Federal Ministry of Education and Research (BMBF) and the Ministry of Culture and Science of the German State of North Rhine-Westphalia (MKW) under the Excellence Strategy of the Federal Government and the Länder, the Deutsche Forschungsgemeinschaft (DFG, projects: GRK 1856, Integrated Energy Supply Modules for Roadbound E-Mobility). Florian Wirsing thanks RWTH Aachen University for financial support through the RWTH Aachen–University of Alberta Junior Research Fellowship.

Declaration of competing interest

The authors have no competing interests to declare that are relevant to the content of this article.

References

[1] Bobzin K, Wietheger W, Jacobs G, Bosse D, Schröder T, Rolink A. Thermally sprayed coatings for highly stressed sliding bearings. *Wear* **458–459**: 203415 (2020)

[2] Chun S M, Khonsari M M. Wear simulation for the journal bearings operating under aligned shaft and steady load during start-up and coast-down conditions. *Tribol Int* **97**: 440–466 (2016)

[3] Sohn C, Andert J, Jolovic D. An analysis of the tradeoff between fuel consumption and ride comfort for the pulse and glide driving strategy. *IEEE Trans Veh Technol* **69**(7): 7223–7233 (2020)

[4] Cai J L, Xiang G, Li S, Guo J A, Wang J X, Chen S A, Yang T Y. Mathematical modeling for nonlinear dynamic mixed friction behaviors of novel coupled bearing lubricated with low-viscosity fluid. *Phys Fluids* **34**(9): 93612 (2022)

[5] Xiang G, Yang T Y, Guo J, Wang J X, Liu B, Chen S A. Optimization transient wear and contact performances of water-lubricated bearings under fluid-solid-thermal coupling condition using profile modification. *Wear* **502–503**: 204379 (2022)

[6] Wodtke M, Litwin W. Water-lubricated stern tube bearing—Experimental and theoretical investigations of thermal effects. *Tribol Int* **153**: 106608 (2021)

[7] Litwin W. Influence of local bush wear on water lubricated sliding bearing load carrying capacity. *Tribol Int* **103**: 352–358 (2016)

[8] Bouyer J, Fillon M, Pierre-Danos I. Influence of wear on the behavior of a two-lobe hydrodynamic journal bearing subjected to numerous startups and stops. *J Tribol* **129**(1): 205–208 (2007)

[9] Hashimoto H, Wada S, Nojima K. Performance characteristics of worn journal bearings in both laminar and turbulent regimes. Part I: Steady-state characteristics. *S L E Trans* **29**(4): 565–571 (1986)

[10] Hashimoto H, Wada S, Nojima K. Performance characteristics of worn journal bearings in both laminar and turbulent regimes. Part II: Dynamic characteristics. *S L E Trans* **29**(4): 572–577 (1986)

[11] Saridakis K M, Nikolakopoulos P G, Papadopoulos C A, Dentsoras A J. Identification of wear and misalignment on journal bearings using artificial neural networks. *Proc Inst Mech Eng Part J* **226**(1): 46–56 (2012)

[12] König F, Sous C, Ouald Chaib A, Jacobs G. Machine learning based anomaly detection and classification of acoustic emission events for wear monitoring in sliding bearing systems. *Tribol Int* **155**: 106811 (2021)

[13] Regis A, Linares J M, Arroyave-Tobon S, Mermoz E. Numerical model to predict wear of dynamically loaded plain bearings. *Wear* **508–509**: 204467 (2022)

[14] Vencl A, Rac A. Diesel engine crankshaft journal bearings failures: Case study. *Eng Fail Anal* **44**: 217–228 (2014)

[15] Ligier J L, Noel B. Friction reduction and reliability for engines bearings. *Lubricants* **3**(3): 569–596 (2015)

[16] Cubillo A, Perinpanayagam S, Esperon-Miguez M. A review of physics-based models in prognostics: Application to gears and bearings of rotating machinery. *Adv Mech Eng* **8**(8): 168781401666466 (2016)

[17] Takabi J, Khonsari M M. On the thermally-induced seizure in bearings: A review. *Tribol Int* **91**: 118–130 (2015)

[18] Hadler J. Tribologische beurteilung und optimierung mischreibungsbeanspruchter radialgleitlager. Ph.D. Thesis. Magdeburg (DE): TU Magdeburg, 1994.

[19] Begelinger A, De Gee A W J. The effect of wear on the performance of statically loaded journal bearings. *S L E Trans* **19**(4): 273–278 (1976)

[20] Rodermund H. Zur auslegung von radialgleitlagern im mischreibungsgebiet. (In German). *Tribologie + Schmierungstechnik* **33**(5): 272–274 (1986)

[21] Maier M, Pusterhofer M, Grün F. Wear simulation in lubricated contacts considering wear-dependent surface topography changes. *Mater Today Proc*, https://doi.org/10.1016/j.matpr.2023.01.424 (2023)

[22] König F, Ouald Chaib A, Jacobs G, Sous C. A multiscale-approach for wear prediction in journal bearing systems—From wearing-in towards steady-state wear. *Wear* **426–427**: 1203–1211 (2019)

[23] Ding N, Li H L, Xin Q, Wu B, Jiang D. Multi-source domain generalization for degradation monitoring of journal bearings under unseen conditions. *Reliab Eng Syst Saf* **230**: 108966 (2023)

[24] König F, Marheineke J, Jacobs G, Sous C, Zuo M J, Tian Z G. Data-driven wear monitoring for sliding bearings using acoustic emission signals and long short-term memory neural networks. *Wear* **476**: 203616 (2021)

[25] Ding N, Li H L, Yin Z W, Zhong N, Zhang L. Journal bearing seizure degradation assessment and remaining useful life prediction based on long short-term memory neural network. *Measurement* **166**: 108215 (2020)

[26] Argatov I, Jin X Q. Time-delay neural network modeling of the running-in wear process. *Tribol Int* **178**: 108021 (2023)

[27] Bote-Garcia J L, Gühmann C. Wear volume estimation for a journal bearing dataset. *Tm Tech Mess* **89**(7–8): 534–543 (2022)

[28] Shutin D, Bondarenko M, Polyakov R, Stebakov I, Savin L. Method for on-line remaining useful life and wear prediction for adjustable journal bearings utilizing a combination of physics-based and data-driven models: A numerical investigation. *Lubricants* **11**(1): 33 (2023)

[29] Dang C, Valdebenito M A, Faes M G R, Wei P F, Beer M. Structural reliability analysis: A Bayesian perspective. *Struct Saf* **99**: 102259 (2022)

[30] König F. *Prognose des Verschleißverhaltens ölgeschmierter Gleitlager*. Aachen (DE): Verlagsgruppe Mainz GmbH, 2020.

[31] Offner G, Knaus O. A generic friction model for radial slider bearing simulation considering elastic and plastic deformation. *Lubricants* **3**(3): 522–538 (2015)

[32] Zhao F Q, Tian Z G, Liang X H, Xie M J. An integrated prognostics method for failure time prediction of gears subject to the surface wear failure mode. *IEEE Trans Reliab* **67**(1): 316–327 (2018)

[33] Conjugate Bayesian analysis of the Gaussian distribution. https://www.cs.ubc.ca/~murphyk/Papers/bayesGauss.pdf, 2007

[34] Gebraeel N, Elwany A, Pan J. Residual life predictions in the absence of prior degradation knowledge. *IEEE Trans Reliab* **58**(1): 106–117 (2009)

[35] Bergmann P, Grün F, Summer F, Gódor I. Evaluation of wear phenomena of journal bearings by close to component testing and application of a numerical wear assessment. *Lubricants* **6**(3): 65 (2018)

Florian KÖNIG. He received his B.S., M.S. (2014), and Ph.D. (2020) degrees in mechanical engineering from the RWTH Aachen University, Germany, focusing on mechanical engineering and tribology. Currently, he is a department head of the tribology group at the Institute for Machine Elements and Systems Engineering, Germany. His research interests include the friction, wear, and lubrication behavior of bearings, surface texturing, condition monitoring, and machine learning methods.